Etude numérique multi-échelle des relations structure-propriétés acoustiques d'une mousse à distribution étendue de tailles de pores

CT. NGUYEN[a], C. PERROT[a], F. DETREZ[a], J. GUILLEMINOT[b]

a. MSME - Laboratoire de Modélisation et Simulation Multi Echelle (Université Paris-Est, 5 Bd Descartes, 77454 Marne-la-Vallée, Cedex 2 - France)
{cong-truc.nguyen, camille.perrot & fabrice.detrez}@u-pem.fr
b. Department of Civil and Environmental Engineering, Duke University, Durham, USA
johann.guilleminot@duke.edu

Résumé

Les mousses acoustiques sont de plus en plus utilisées dans l'industrie en remplacement des milieux fibreux pour des raisons de santé notamment. Leurs propriétés acoustiques dépendent fortement de leurs microstructures (distribution de taille de pores, présence de membranes). L'objectif de ce travail est d'étudier l'influence d'une distribution étendue de tailles de pores sur les propriétés acoustiques et élastiques. La microstructure des mousses est reconstruite en trois étapes. La première étape consiste en la génération d'un empilement aléatoire de sphères, généré par la méthode des éléments discrets. Ensuite, une tessellation de Laguerre à partir des centres et des rayons des sphères est réalisée pour construire le squelette de la mousse. Finalement, les bords de Plateau ayant une section triangulaire concave d'épaisseur variable, sont obtenus par minimisation d'énergie de surface à l'aide du logiciel Surface Evolver. Les propriétés acoustiques sont calculées à l'aide de simulations par la méthode des éléments finis.

Abstract

An acoustic foam is utilized increasingly in industrial by replacing the fibrous layer because of particularly a health reason. Its acoustic properties depend heavily on its microstructures (pore size's distribution, membrane presence). The aim of this work is to study the influence of an extended of pore size's distribution on its properties acoustic and elastic. The microstructure of the acoustic foam is created in three steps. Firstly, by using the discrete element method, a random stack of sphere is generated. After that, a tessellation of Laguerre from the center and radius of the spheres is carried out to build a foam skeleton. Finally, the Plateau borders, that have a concave triangular section of a variable thickness, is obtained by a minimizing of surface energy with the help of a Surface Evolver software. A simulation with the help of the finite elements method evaluates the properties acoustic.

Mots clefs : Mousses, propriétés acoustiques, relations structure, propriétés, stratégie numérique, multi-échelle

1   Introduction

Nowadays, cellular foams are a materials which are utilized in a lot of domains : structure, thermal, or acoustical. Particularly, an acoustic foam is utilized increasingly in industrial by replacing the fibrous layer because of many reasons that the most important of its is health reason. The microstructure of acoustic foam influences heavily on its acoustic properties via its parameters : pore size distribution, membrane presence and so on. The study of the microstructure of the acoustic foam has been carried out by several works. The aim of its to validate the transport parameters (viscous and thermal permeability, viscous and thermal tortuosity, ...) together with the sound absorption coefficient by introducing the input parameters on a microstructure model. The works are realized with a membrane fully opened or fully closed. In 2012, Hoang et al. [25] are studied the microstructure by using the Kelvin's cellular by considering a fully open foam with a uniform membrane closure ratio. Recently, based on a Kelvin's cellular taking into account both of the proportion of closed window and the closure ratio, Trinh et al. [26] gave a good estimates of macroscopic parameters.

In this paper, we focus on a influence of a pore size distribution on a acoustic properties of the foams. In acoustic domain, the previous works has been studied with a pore-size distribution constant by using the ideal periodic unit cell (PUC) [26, 8, 20, 25]. However, the variation of pore size extended distribution has been carried out on a elastic problem which are characterized by a foam closed or opened completely [22]. Thus, this work presents a microstructure model of the acoustic foam which the pore size's distribution satisfied a Gamma's law. Firstly, a spheres packing is created obeying a Gamma distribution by using the discrete element method (DEM). An algorithm using a software *voro++* and together the parameters of a centers and a radius of the random multi-sized are applied to generate a random Laguerre tessellation. After that, a microstructure model are finalized by creating the borders form the random Languerre tesselation. By using the algorithm for the foam relaxation, this work allows us to obtain a microstructure of an acoustic foams which is satisfied a Plateau's law.

A calculations of acoustic properties are realized with some of examples : calculation of visco-thermal parameters, calculation of sound absorbing properties. The parameters of both of calculations are shown in an illustration of numerical results. In this part, the permeability is satisfied a Sampson equation. In the future works, we will focus on a validation of methodologies for another parameters.

2   Microstructures model

2.1   Random multi-sized dense spheres packing

According to the literature, there are various methods can be exploited to generate the random dense multi-sized spheres packing, e.g. sequential-deposition, molecular dynamics and collective rearrangement methods [7]. In this work, we use the discrete element method (DEM) with the open source code LIGGGHTS [27]. In this method, N spherical particles with arbitrary radius distributions are randomly generated no velocity initial within a cube domain. In the initial state, we have a system of overlapping spheres. The spheres then move because of a frictional force dependent of distance between two spheres, defined by hertz model [28]. In order to avoid boundary effects, the periodic boundary conditions are used. When steady state conditions are reached (i.e. zero velocity for the entire set of spheres), the simulation stops. The dimensions of cube domain are chosen to have a desired volume fraction of packing. In this work, the desired volume fraction is $f = 70\%$, we have a dense system of spheres. Fig. 1

illustrates a packing of 100 random spheres, they have the volume satisfying a distribution of Gamma.
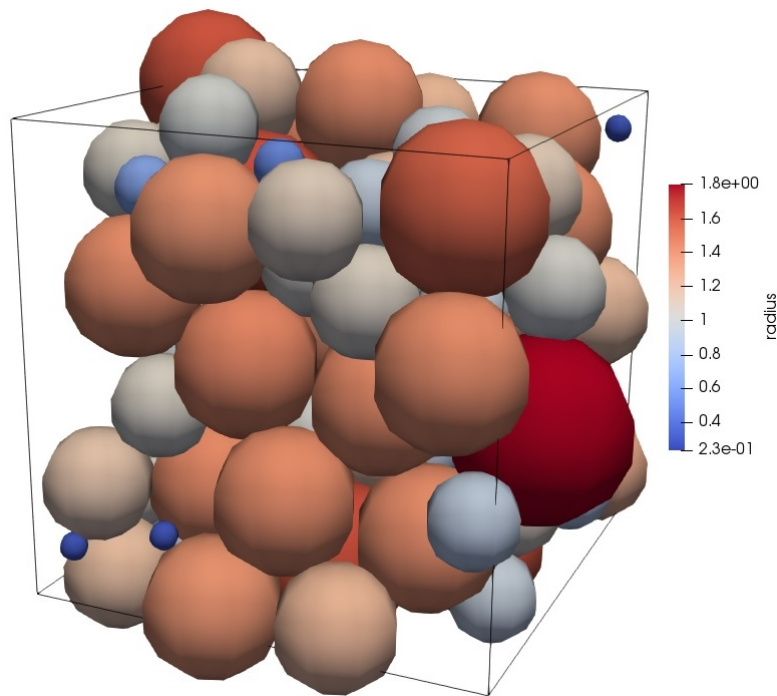

Figure 1: A spheres packing with $CV_{SP} = 0.7$ for $N = 100$ and $f = 70\%$.

2.2 Random Laguerre tessellation

Random Laguerre tessellations is a weighted generalization of the well-known Voronoi tessellation. A random Laguerre tessellation in $\mathbb{R}^3$ can be defined as follows [2]: given a set of random spheres $S = \{s_i(x_i, r_i), x_i \in \mathbb{R}^3, r_i > 0, i \geq 1\}$ in $\mathbb{R}^3$, x_i and r_i is the center and radii of sphere s_i, respectively. The 3-dimensional space is filled by a system of convex polytopes, so-called Laguerre cells $C = \{c_i, i \geq 1\}$, which is defined as

$$c_i = \{x \in \mathbb{R}^3 : \|x - x_i\|^2 - r_i^2 \leq \|x - x_j\|^2 - r_j^2, \forall j \neq i\}, \tag{1}$$

where $\|.\|$ denotes the Euclidean norm in $\mathbb{R}^3$. If all spheres have same radii, the Voronoi tessellation is obtained. Because cell facets are not forced to be equidistant to the cell generators (i.e. center of sphere), the Laguerre tessellation allows to generate a more wider range than the Voronoi tessellation. Note that, in $\mathbb{R}^3$, the Laguerre tessellations are a *normal* tessellation [17], it means that each facet is intersection in exactly 2 cells and each edge is intersection in exactly 3 facets. For a detailed discussion of Laguerre tessellations, the readers are referred to [17, 2].

In this work, the Laguerre tessellation using the centers and the radius of the random multi-sized dense spheres packing, is generated with help of the open-source software *voro++* [24] and imposing periodic boundary conditions at the border of the cube domain in order to avoid boundary effects. Fig. 2 illustrate a Laguerre tessellation of a packing of 100 random spheres.
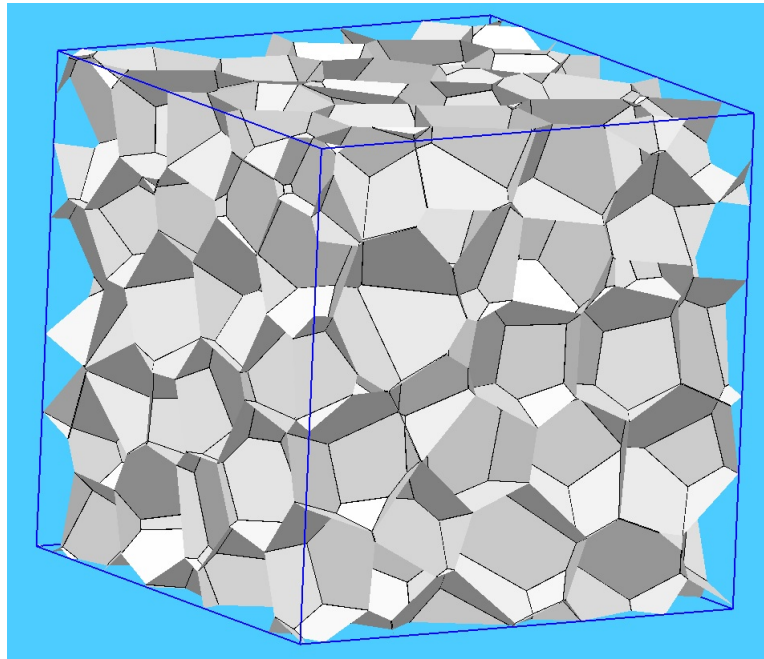
Figure 2: A Laguerre tessellation based on a SP with $CV_{SP} = 0.7$ for $N = 100$ and $f = 70\%$.

2.3   Plateau borders

In the case of dry foam, where the liquid fraction is almost zero, the structure is set of polyhedral cells that are bounded by slightly curved thin films. At equilibrium state, the structure satisfies the laws of Plateau [21]: (1) the films always meet in threes along an edge and they must do so at an angle of $120°$, (2) only four edges meet at a vertex, and they do so at an angle of $\arccos(-1/3) \approx 109.47°$, (3) the liquid films are the surfaces of constant mean curvature. A wet foam is a foam where the liquid fraction is more than one percent, most of its liquid is contained in so called Plateau borders. They have a concave triangular section and a locally varying thickness, which is maximum at the junction and minimum at the center. In the case of solid polymer foams, we can consider they are as a liquid that was frozen and thus shares many geometric properties of a wet foam [18]. In this context, the terms Plateau borders are referred to as struts and films.

Forget about the curvature of the films, the dry foams that is based on a normal tessellation is dictated by topology induced by Plateau's laws. A foam satisfied fully Plateau's laws can be obtained by a 'relaxed' Laguerre tessellation [1, 14]. Andrew Kraynik [12, 13] developed a algorithm for the foam relaxation. In this work, based on this algorithm, we use the random Laguerre tessellation to simulate the polymer solid foams by replacing the edges to struts of section triangular. After that, the system of cells and struts is relaxed until Plateau's laws are satisfied. The numerical procedure for relaxing the tessellation is based on the Surface Evolver software developed by Ken Brakke [6]. Fig. 3 illustrates a system of Plateau borders generated by Surface Evolver software.

2.4   Identification of pore's size distribution

The pore size distribution of real foams is identified with the cell volume distribution of the Laguerre tessellation via the mean of pore volume $\overline{V}$ and their variation coefficient $CV = \delta/\overline{V}$, where δ is the standard deviation of pore volume.
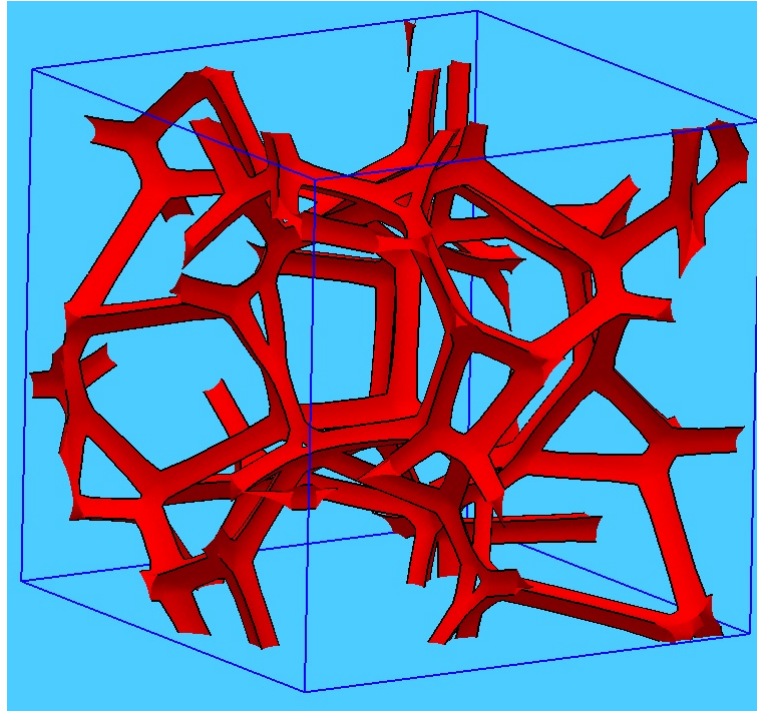
Figure 3: Plateau borders

The properties of random spheres packing, $\overline{V}_{SP}$ and CV_{SP}, must be choose such as the proprieties of the Laguerre tessellation and of the foams are identified, it means $\overline{V}_{LT} = \overline{V}_{foam}$ and $CV_{TL} = CV_{foam}$. Easy to see, $\overline{V}_{SP} = f \times \overline{V}_{TL}$ where f is the volume fraction of the spheres packing. Fan et al. [9] and C.Redenbach [23] construed the graphical relation between the variation coefficient of the spheres packing and that of the corresponding Laguerre tessellation for a system of $N = 10000$ spheres. Here, because of the calculation cost limitation (the calculation cost increases rapidly with number of spheres or number of cells), we fix $N = 100$ spheres and reconstruct the graphical relation. More precise, $N = 100$ spheres with the volume distribution follow a Gamma distribution are generated inside a cube domain such as the volume fraction $f = 70\%$, we keep the volume mean constant and the variation coefficient is chosen between 0.2 and 1.6 at intervals of 0.2. Ten realizations are generated for each set of parameters. The values observed for the CV of the cell volumes are plotted in Fig. 4. In order of comparison, the 3 dotted lines corresponding to a case of $V = 40\%, 50\%, 60\%$ are shown in the Fig. 4 [23]. Thanks to this figure, we can choose the value of CV_{SP} to have the desired value of CV_{LT}.

3 Calculations of acoustic properties

3.1 Calculations of visco-thermal parameters

The set of eight transport parameters is computed by using the hybrid micro-macro method which combines finite element modeling and semi-phenomenological models (JCA and JCAL). This method is used and validated in the work of Perrot et al. [19]. The two first parameters, purely geometrical, (ϕ, Λ') are estimated by direct spatial integration on the volume and surface elements of the microstructure. The open porosity ϕ is defined as the fraction of the interconnected pore fluid volume to the total bulk volume of the porous medium, the thermal characteristic length Λ' is defined as twice the ratio of the total pore volume to its surface area. The six remaining transport properties are computed by solving the local
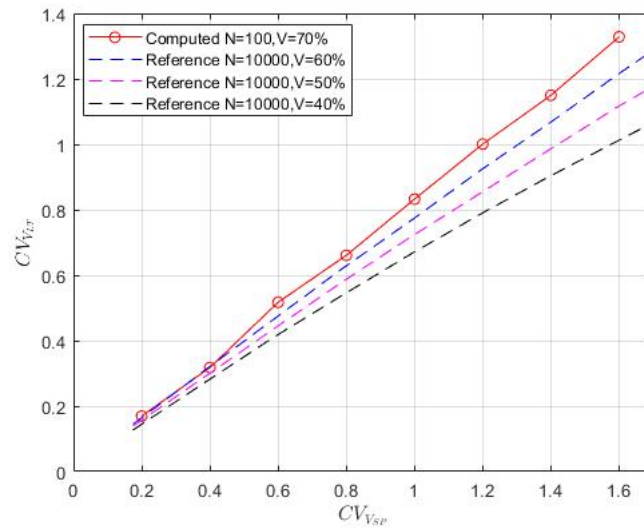
Figure 4: Variation coefficient of the volumes of the Laguerre cells CV_{LT} versus CV_{SP}.

equations governing the asymptotic frequency-dependent visco-thermal dissipation phenomena at the microscopic scale.

The static viscous permeability k_0 (or the static resistivity σ where $\sigma = k_0/\mu$ with μ is the dynamic viscosity of the fluid) reflects the ability to oppose a flow of a material. The static viscous tortuosity α_0 characterizes the dispersion of the microscopic velocity field for quasi-steady movements of the viscous fluid flow. Both of these parameters are computed from the Stokes problem in the fluid phase [10, 3]:

$$\mu\Delta\mathbf{v} - \nabla p = -G \quad in \quad \Omega_f$$
$$\nabla\mathbf{v} = 0 \quad in \quad \Omega_f$$
$$\mathbf{v} = 0 \quad on \quad \partial\Omega$$
$$\mathbf{v} \quad and \quad p : \quad \Omega - periodic$$

where $\mathbf{v}$, p are the velocity and pressure of the fluid, respectively. G is the macroscopic pressure gradient acting as a source term. It can be shown that the local field of the static viscous permeability $\mathbf{k}_0$ is obtained from the local velocity field as $\mathbf{v} = -\frac{\mathbf{k}_0}{\mu}G$. The components of the static viscous permeability tensor are calculated:

$$k_{0_{ij}} = \phi\left\langle\mathbf{k}_{0_{ij}}\right\rangle \tag{2}$$

and the components of the tortuosity tensor are obtained from:

$$\alpha_{0_{ij}} = \frac{\left\langle\mathbf{k}_{0_{pi}}\mathbf{k}_{0_{pj}}\right\rangle}{\left\langle\mathbf{k}_{0_{ii}}\right\rangle\left\langle\mathbf{k}_{0_{jj}}\right\rangle} \tag{3}$$

The symbol $\langle.\rangle$ indicates a fluid-phase average.

In the high frequency range, the fluid tends to behave as a perfect one. The potential flow problem is

formally identical to the electrical conduction problem [5, 4]:

$$\nabla.\mathbf{E} \quad with \quad \mathbf{E} = -\nabla\varphi + \mathbf{e} \quad in \quad \Omega_f$$

$$\mathbf{E}.\mathbf{n} = 0 \quad on \quad \partial\Omega$$

$$\varphi: \quad \Omega - periodic$$

where $\mathbf{e}$ is a given macroscopic electric field, $\mathbf{E}$ is the solution of the boundary problem having $-\nabla\varphi$ as a fluctuating part, and $\mathbf{n}$ is the unit normal to the boundary of the fluid phase. The viscous characteristic length Λ and the high frequency tortuosity α_∞ are calculated by:

$$\Lambda = \frac{2\int_{\Omega_f}\mathbf{E}^2 dV}{\int_{\partial\Omega}\mathbf{E}^2}dS, \quad \alpha_\infty = \frac{\langle\mathbf{E}^2\rangle}{\langle\mathbf{E}\rangle^2} \tag{4}$$

The static thermal permeability k_0' and the static thermal tortuosity α_0' can be computed by solving the thermal conduction problem where the solid skeleton is considered a thermostat:

$$\nabla^2 u = -1 \quad in \quad \Omega_f$$

$$u = 0 \quad on \quad \partial\Omega$$

where u is the local temperature field. The mean value of the excess temperature field in the fluid phase is directly related to the definition of the thermal permeability:

$$k_0' = \langle u \rangle \tag{5}$$

The static thermal tortuosity α_0' is given by:

$$\alpha_0' = \frac{\langle u^2 \rangle}{\langle u \rangle^2} \tag{6}$$

3.2   Calculations of sound absorbing properties

Follow the equivalent-fluid approach, a rigid porous medium is substituted by an effective fluid, this fluid can be characterized by the effective density $\rho_{ef}(\omega)$ and effective bulk modulus $K_{ef}(\omega)$ as follows [11, 15]:

$$\rho_{ef}(\omega) = \rho_0\alpha_\infty\left[1 + \frac{f(\varpi)}{\varpi}\right] \tag{7}$$

$$K_{ef}(\omega) = K_a\left[\gamma - (\gamma - 1)\left[1 + \frac{f'(\varpi'))}{j\varpi'}\right]^{-1}\right]^{-1} \tag{8}$$

where ρ_0 is the air density, K_a is the adiabatic bulk modulus of air, and γ is its specific heat ratio. ϖ and ϖ' are dimensionless frequencies, $f(\varpi)$ and $f'(\varpi')$ are shape functions:

$$\varpi = \frac{\omega}{\nu}\frac{k_0\alpha_\infty}{\phi}, \quad \varpi' = \frac{\omega}{\nu'}\frac{k_0'}{\phi} \tag{9}$$

$$f(\varpi) = \sqrt{1 + \frac{M}{2}j\varpi}, \quad f'(\varpi') = \sqrt{1 + \frac{M'}{2}j\varpi'} \tag{10}$$

$$M = \frac{8k_0\alpha\infty}{\Lambda 2 2\phi}, \quad M' = \frac{8k_0'}{\Lambda'^2\phi} \tag{11}$$

In these equations, $\nu' = \nu/Pr$ with ν is the kinematic viscosity and Pr is the Prandtl number, M and M' are dimensionless shape factors.

The properties of the equivalent homogenenous porous medium are characterized by the equivalent density $\rho_{eq}(\omega)$ and equivalent bulk modulus $K_{eq}(\omega)$:

$$\rho_{eq} = \frac{\rho_{ef}(\omega}{\phi}, \quad K_{eq}(\omega) = \frac{K_{ef}(\omega)}{\phi} \tag{12}$$

Assuming plane wave solutions varying as $exp\left[j(\omega t - q_{eq}(\omega)x\right]$, where $q_{eq}(\omega)$ is the wave number of the equivalent fluid medium. The wave number and the characteristic impedance of the equivalent fluid medium are determined by:

$$q_{eq}(\omega) = \omega\sqrt{\frac{\rho_{eq}(\omega)}{K_{eq}(\omega)}}, \quad Z_{c_{eq}} = \sqrt{\rho_{eq}(\omega)K_{eq}(\omega)} \tag{13}$$

The sound absorption coefficient at normal incidence of a porous medium of thickness d backed by a rigid wall is evaluated by:

$$\alpha_n = 1 - \left(\frac{Z_n - 1}{Z_n + 1}\right)^2 \tag{14}$$

with Z_n the effective normal impedance on the free face of the excited material:

$$Z_n = -j\frac{Z_{c_{eq}}}{Z_0}\cot(q_{eq}d) \tag{15}$$

where Z_0 is the characteristic impedance of air.

3.3   Illustration of numerical results and scaling laws

3.3.1   Scaling laws

First, we check numerically that a generated foam structure corresponding to a given monodisperse pore size with a varying R_0 follows a scaling corresponding to the Sampson law [16] :

$$\left(\frac{k_0}{D^2}\right) \propto \left(\frac{R_0}{D}\right)^3 \tag{16}$$

where : k_0, R_0 and D are permeability, mean of aperture size and size pore respectively. The numerical results are fitted by the Sampson's law and are shown in the Fig. 5. In this figure, $\frac{k_0}{D^2}$ is proportional to $\left(\frac{R_0}{D}\right)^3$ by a factor $\sigma_w = 1.527$. The permeability is computed by solving the Stoke's problem. We note that, in this example, there are 10 pores of size constant.
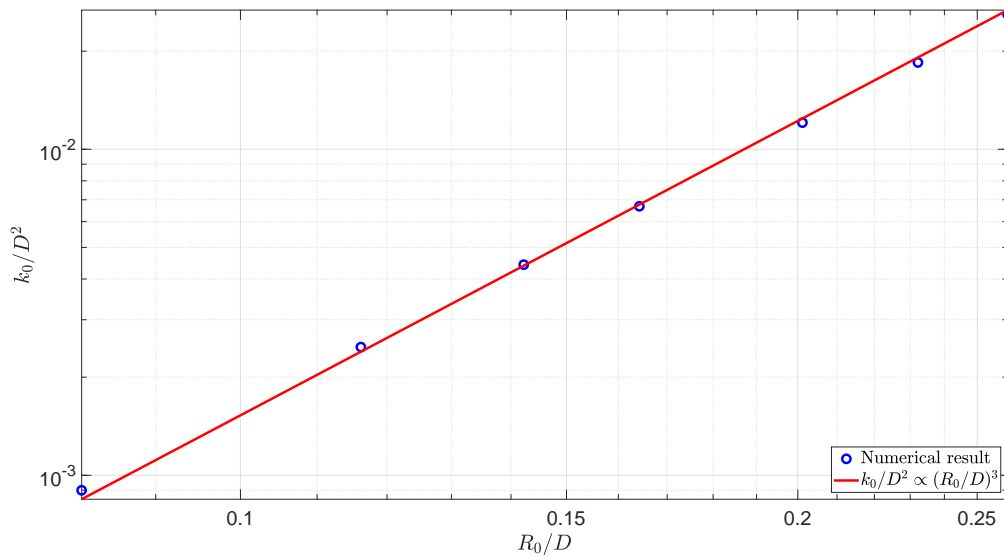
Figure 5: Numerical results and Sampson's law fit

3.3.2   Illustration examples

The transport parameters and the absorption coefficients are calculated in two cases of monodisperse pore S_1 and S_2 with different of the mean of closure with ratio $\langle r_c \rangle$ which is calculated as follows :

$$\langle r_c \rangle = \left\langle 1 - \frac{A_{op}}{A_w} \right\rangle \tag{17}$$

where : A_{op} and A_w are the aire of the open part and the total aire of the windows respectively. Figures 6a and 6b show the geometry and mesh of the microstructure model in the sample S_2.

The nature of the foam is anisotropic and is taked into account this microstructure model. Thus, the acoustic properties of the foam are different in three directions and are shown in the Table 1.

		ϕ	$D_b(\mu m)$	$\langle r_c \rangle$	$k_0(\times 10^{-10}m^2)$	$k_0'(\times 10^{-10}m^2)$	$\Lambda(\mu m)$	$\Lambda'(\mu m)$	α_∞
S_1	x	0.983	810	0.33	121	326	543	811	1.05
	y	0.983	810	0.33	116	326	534	811	1.06
	z	0.983	810	0.33	113	326	541	811	1.05
	Avg	0.983	810	0.33	117	326	539	811	1.05
S_2	x	0.983	810	0.65	46	233	352	620	1.16
	y	0.983	810	0.65	44	233	352	620	1.16
	z	0.983	810	0.65	42	233	338	620	1.16
	Avg	0.983	810	0.65	44	233	347	620	1.16

Table 1: Transport parameters in two examples

The absorption coefficient of two examples are plotted in the Fig. 7 in the frequency domain. We see that, in the high frequency, the absorption coefficient of the sample S_1 is superior than the sample S_2 because of the influence of the closure ratio.

(a)   (b)
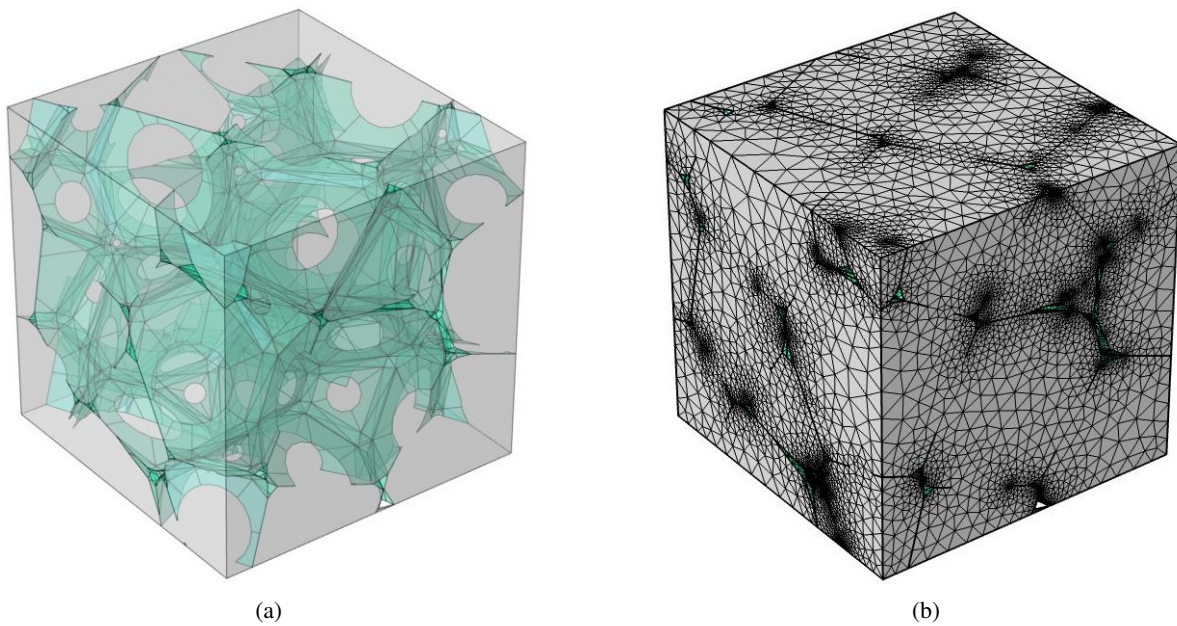
Figure 6: Geometry and mesh of sample S_2
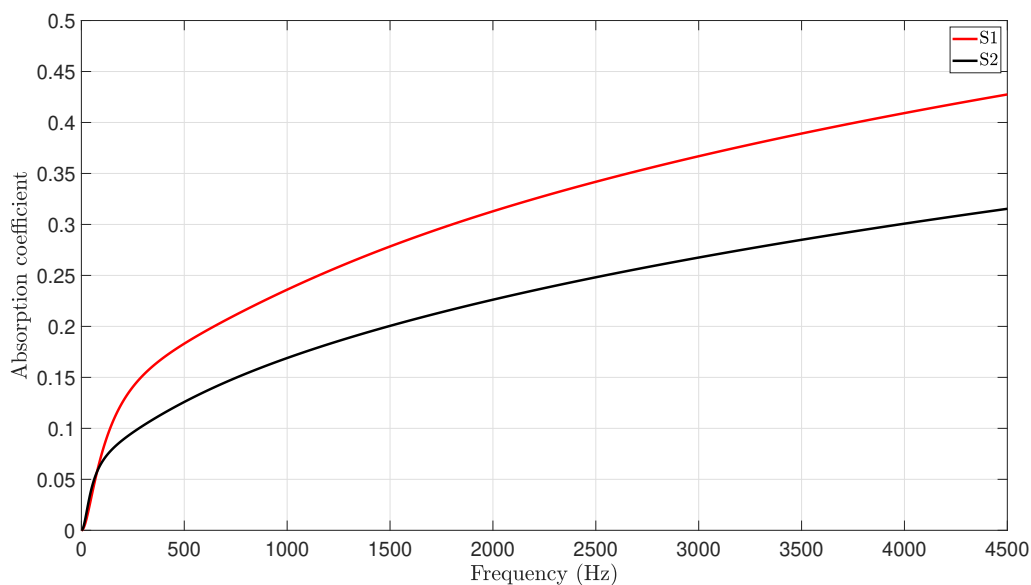
Figure 7: Comparison of absorption coefficient in two case S_1 and S_2 with the same thinkness $20mm$

4   Conclusions

In this study, a microstructure model of an acoustic foam has been developed. This model is created by using a Laguerre tessellation based on random sphere packing and together Plateau's border geometry. By taking into account a size pore distribution and a membrane presence, this model allows us to study the influences on a acoustic properties. The numerical application has been carried out by the calculations of visco-thermal parameters and sound absorbing coefficient. The illustration of numerical results shows the effect of the aperture size on the permeability and is obeyed the Sampson's law. In the future works, this model can be used by taking into account the proportion of closed window and the closure

ratio to study the multi-dispersed size foams.

Acknowledgements

References

[1] Fred Almgren. Computing soap films and crystals. *Computing Optimal Geometries*, pages 3–5, 1991.

[2] Franz Aurenhammer. Power diagrams: properties, algorithms and applications. *SIAM Journal on Computing*, 16(1):78–96, 1987.

[3] Jean-Louis Auriault, Lionel Borne, and René Chambon. Dynamics of porous saturated media, checking of the generalized law of darcy. *The Journal of the Acoustical Society of America*, 77(5):1641–1650, 1985.

[4] Claude Boutin and Christian Geindreau. Estimates and bounds of dynamic permeability of granular media. *The Journal of the Acoustical Society of America*, 124(6):3576–3593, 2008.

[5] Claude Boutin and Christian Geindreau. Periodic homogenization and consistent estimates of transport parameters through sphere and polyhedron packings in the whole porosity range. *Physical review E*, 82(3):036313, 2010.

[6] Kenneth A Brakke. The surface evolver. *Experimental mathematics*, 1(2):141–165, 1992.

[7] Larysa Burtseva, Benjamin Valdes Salas, Rainier Romero, and Frank Werner. *Multi-sized sphere packings: models and recent approaches*. Univ., Fak. für Mathematik, 2015.

[8] Fabien Chevillotte and Camille Perrot. Effect of the three-dimensional microstructure on the sound absorption of foams: A parametric study. *The Journal of the Acoustical Society of America*, 142(2):1130–1140, 2017.

[9] Zhigang Fan, Yugong Wu, Xuanhe Zhao, and Yuzhu Lu. Simulation of polycrystalline structure with voronoi diagram in laguerre geometry based on random closed packing of spheres. *Computational materials science*, 29(3):301–308, 2004.

[10] Christian Geindreau Jean-Louis Auriault, Claude Boutin. *Homogenization of Coupled Phenomena in Heterogenous Media*. Wiley-ISTE, 2009.

[11] David Linton Johnson, Joel Koplik, and Roger Dashen. Theory of dynamic permeability and tortuosity in fluid-saturated porous media. *Journal of fluid mechanics*, 176:379–402, 1987.

[12] Andrew M Kraynik. Foam structure: from soap froth to solid foams. *MRS bulletin*, 28(4):275–278, 2003.

[13] Andrew M Kraynik, Douglas A Reinelt, and Frank van Swol. Structure of random monodisperse foam. *Physical Review E*, 67(3):031403, 2003.

[14] Rob Kusner and John M Sullivan. Comparing the weaire-phelan equal-volume foam to kelvin's foam. *Forma*, 11(3):233–242, 1996.

[15] Denis Lafarge, Pavel Lemarinier, Jean F Allard, and Viggo Tarnow. Dynamic compressibility of air in porous structures at audible frequencies. *The Journal of the Acoustical Society of America*, 102(4):1995–2006, 1997.

[16] V Langlois, VH Trinh, C Lusso, Camille Perrot, X Chateau, Y Khidas, and O Pitois. Permeability of solid foam: Effect of pore connections. *Physical Review E*, 97(5):053111, 2018.

[17] Claudia Lautensack and Sergei Zuyev. Random laguerre tessellations. *Advances in applied probability*, 40(3):630–650, 2008.

[18] André Liebscher. *Stochastic modelling of foams*. Fraunhofer Verlag, 2014.

[19] Camille Perrot, Fabien Chevillotte, and Raymond Panneton. Dynamic viscous permeability of an open-cell aluminum foam: Computations versus experiments. *Journal of Applied Physics*, 103(2):024909, 2008.

[20] Camille Perrot, Fabien Chevillotte, Minh Tan Hoang, Guy Bonnet, François-Xavier Bécot, Laurent Gautron, and Arnaud Duval. Microstructure, transport, and acoustic properties of open-cell foam samples: Experiments and three-dimensional numerical simulations. *Journal of Applied Physics*, 111(1):014911, 2012.

[21] Joseph Plateau. *Statique expérimentale et théorique des liquides soumis aux seules forces moléculaires*, volume 2. Gauthier-Villars, 1873.

[22] C Redenbach, I Shklyar, and H Andrä. Laguerre tessellations for elastic stiffness simulations of closed foams with strongly varying cell sizes. *International Journal of Engineering Science*, 50(1):70–78, 2012.

[23] Claudia Redenbach. Microstructure models for cellular materials. *Computational Materials Science*, 44(4):1397–1407, 2009.

[24] Chris Rycroft. Voro++: A three-dimensional voronoi cell library in c++. Technical report, Lawrence Berkeley National Lab.(LBNL), Berkeley, CA (United States), 2009.

[25] Minh Tan Hoang and Camille Perrot. Solid films and transports in cellular foams. *Journal of applied physics*, 112(5):054911, 2012.

[26] Van Hai Trinh, Vincent Langlois, Johann Guilleminot, Camille Perrot, Yacine Khidas, and Olivier Pitois. Tuning membrane content of sound absorbing cellular foams: Fabrication, experimental evidence and multiscale numerical simulations. *Materials & Design*, 162:345–361, 2019.

[27] Gregor D. Wehinger, Thomas Eppinger, and Matthias Kraume. Detailed numerical simulations of catalytic fixed-bed reactors: Heterogeneous dry reforming of methane. *Chemical Engineering Science*, 122:197 – 209, 2015.

[28] HP Zhang and HA Makse. Jamming transition in emulsions and granular materials. *Physical Review E*, 72(1):011301, 2005.